PERFORMANCE OF UNDERWATER WIRELESS OPTICAL IoT NETWORKS USING CDMA

Nguyen Van Thang[*], Pham Thi Thuy Hien[#]
[*]The University of Aizu
[#]Posts and Telecommunications Institute of Technology

Abstract: The reliability of an underwater wireless optical communication (UWOC) network is seriously impacted by oceanic turbulence and beam misalignment between transmitters (Tx) and receivers (Rx). Also, the performance of UWOC systems can be affected by oceanic turbulence-induced fading due to fluctuations in the water refractive index as a result of variations in pressure, water, and temperature. In this work, we investigate the performance of a vertical UWOC link subject to propagation loss, beam spreading and pointing loss, and oceanic turbulence. Furthermore, we investigate optical code-division multiple-access (CDMA), which is utilized to enable asynchronous and simultaneous data transmission between sources (e.g., underwater sensors, submarines, divers, etc.) and the destination, which can be a ship, buoys, unmanned underwater vehicles, and so on. This study is based on an accurate mathematical framework for link modeling while taking into account realistic Tx/Rx and channel parameters under the effects of the oceanic turbulence and beam spreading loss conditions. In addition, we provide an analytical expression for calculating the bit error rate (BER). Moreover, the necessity of optimal Tx/Rx parameter selection is demonstrated to satisfy the quality of service such as BER. The presented results give valuable insight into the practical aspects of the deployment of UWOC systems using CDMA.

Keywords: Underwater wireless optical communications (UWOC), code division multiple access (CDMA), oceanic turbulence.

I. INTRODUCTION

Nowadays, demands for underwater communication networks are increasing due to the ongoing expansion of related human activities, such as environmental monitoring, offshore oil field exploration, port security, etc. Such networks should enable communication with underwater vehicles or harvest data from underwater sensors. Within the underwater Internet of Things (IoTs) paradigm, we are concerned with a diverse range and data-rate requirements with a challenging issues of unpredictable propagation environment. Within this context, underwater wireless optical communication (UWOC) is considered an efficient complementary technology to acoustic communications for short-to-moderate link ranges, allowing for high-speed, low-latency data transmission in such networks [1–3]. In practice, UWOC link performance is impacted by several parameters, including water absorption and scattering [4–6], solar background noise [7, 8], oceanic turbulence [9], and pointing errors (PEs) [10–12], thus necessitating efficient techniques for mitigating these effects. In addition to analyze deterministic losses, e.g., propagation loss, beam spreading loss, this work focuses on the impacts of oceanic turbulence, which dominates the dynamic performance of underwater links. We further consider the appropriate selection of transmitter (Tx)/receiver (Rx) parameters to minimize the impact of random channel effects.

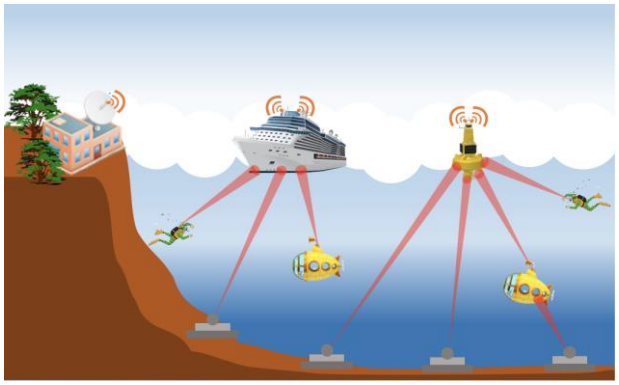

Fig. 1. Example of underwater wireless optical communications supporting multiple users.

Recently, UWOC systems have been attracted from both academia and industry because radio-frequency (RF) energy is highly attenuated by seawater [13–15]. This research was inspired by the need to design an underwater wireless optical network with the multiple-access capability to enable possible communication among various users such as unmanned underwater vehicles (UUVs), underwater sensors, submarines, ships, buoys, and divers. These classes of communication networks are expected to play important roles in investigating climate change, monitoring biological, biogeochemical, evolutionary, and ecological changes in the sea, ocean, and lake environments, tracking pollutants flowing in from

Contact author: Pham Thi Thuy Hien
Email: hienptt@ptit.edu.vn
Manuscript received: 14/7/2022, revised: 14/8/2022, accepted: 22/8/2022.

land and helping to control and maintain oil production facilities and harbors. Among all multiple-access schemes such as time division (TDMA), wavelength division (WDMA), spatial division (SDMA), and code division multiple access (CDMA), CDMA is interested in UWOC network due to its fully asynchronous random-access ability without a central network management protocol, which is highly suitable and desirable in an underwater environment. In addition, CDMA helps in achieving maximum throughput and aims for secure transmission of the message [16]. As for network security, CDMA mixes the data that constitutes the message with pseudo-random bits, resulting in a signal that appears nonsense to an outsider. CDMA provides secure communications for the military, for example, as the technology resists interference from jamming and other threats.

In recent years, there are number of works focusing on studying the UWOC by applying CDMA technique [17–19]. The authors in [17] investigated the structures, principles, and performance of an underwater wireless OCDMA network in various water types. The authors implemented their proposed network on field programmable gate arrays and made an experimental setup to evaluate the framework in a laboratory water tank. In similar system, localization and positioning scheme based on UWOC network using CDMA is studied in [18]. Last but not least, the characterization of the relay-assisted UWOC using CDMA networks over turbulent channels was considered in [19]. In addition to investigating the log-normal fading coefficient, the authors also inspect underwater channels' scattering and absorption effects. However, those works did not consider the beam spreading and pointing error loss, which is severely affected to the OWC systems.

Motivated from that perspective, this paper aims to design and evaluate the performance of the UWOC system using CDMA, as shown in Fig. 1. The main contributions of this paper present as follow:

- Firstly, optical CDMA is deployed at sources, e.g., underwater sensors, submarines, divers, etc., so as to exchange data asynchronously and simultaneously among all sources using a single wavelength with low multiple access interference. The application scenario can be implemented based on our proposed UWOC access network. In particular, the data are exchanged between one destination and multiple access sources. The destination equipped with multiple transceivers is responsible for transferring the data between a core network and access networks.
- A CDMA technique is employed in our work to mitigate multiple-access interference (MAI) efficiently, which can reduce the system's capacity and increase its bit error rate (BER). In consideration of the fading channel, the knowledge of both MAI and noise statistics plays a vital role in various applications such as designing an optimum receiver based on maximum likelihood (ML) detection, evaluating the bit error rate, In this work, we focus on evaluating the bit error rate.
- Mathematical expressions for BER of the proposed UWOC access network are derived by taking into account the impact of propagation loss, oceanic turbulence, beam spreading and pointing loss, MAI, and receiver noise. Based on the obtained mathematical expressions, the network performance is investigated versus various system parameters to evaluate the feasibility of the proposed UWOC network. From the network design perspective, numerical results are useful in designing the UWOC network and provide selected parameters to satisfy the quality of service such as BER.

The rest of the paper is organized as follows. Section II introduces the system model. Then, the comprehensive UWOC channel modeling is elaborated in section III. The performances of our considered system will be analyzed in section IV. Section V demonstrates the numerical results and discussions. Finally, the study is summarized in Section VI.

II. SYSTEM MODEL

Our proposed network model is an UWOC access network that includes K sources, which can be sensors, submarine, divers, etc. They connect to the destination, e.g., ship or floating sensor as shown in Fig. 1. Each source is assigned a unique code. In the first time slot, all sources encode their packets with optical codes and send encoded signals to the destination, where they are combined at chip level in optical domain. The following parts will explain the whole process in detail with specific mathematical expressions of signals.

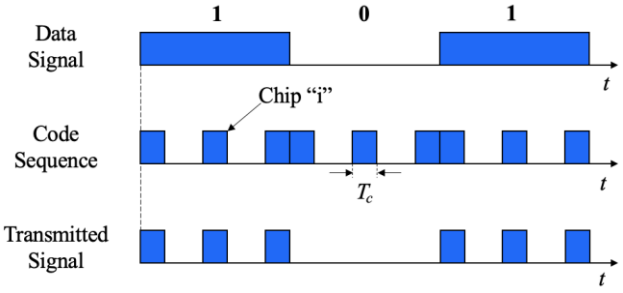

Fig. 2. Example of underwater optical CDMA encoding scheme.

First, the binary data at each GS are encoded with its code sequence. Accordingly, bit-level electrical waveform is converted to chip-level optical waveform as shown in Fig. 2. Source #k sends an optical chip sequence $A_k(t)$ representing bit "1," whereas the signal is not transmitted for the case of bit "0." $A_k(t)$ can be expressed for source #k as

$$A_k(t) = \sum_{i=1}^{L} c_{k,i}(t)\, p(t - iT_c)\sqrt{P_k^{(T)}} \times \exp\left[j(\omega_c t + \varphi_k) \right], \quad (1)$$

where L is the code length using optical spread spectrum, $c_{k,i}(t)$ is the "i"-th chip in the code sequence with the code c_k length L ($1 \le i \le L$). Moreover, $p(t - iT_c)$ is definded as the rectangular pulse with the "1" value for $t \in [0,\ T_c]$. T_c is the chip duration, $P_k^{(T)}$ is the transmitted power per chip of source #k. The optical carrier frequency and phase are denoted as ω_c and φ_k, respectively. Figure 2 shows a prime code sequence with the code length L = 9 and the code weight, i.e., the number of optical pulses in a code

sequence, ρ = 3. Next, the signal is transmitted to the destination via UOWC channel.

III. CHANNEL MODELING

This section is an in-depth introduction of underwater UWOC channel model. The channel coefficient, h, is modeled as

$$h = h_{k,l} h_{k,bl} h_t, \tag{2}$$

where $h_{k,l}$ and $h_{k,bl}$ denote propagation loss and beam spreading loss, which are considered as a deterministic value. And, h_t represents the effect of turbulence, which is studied as a random variable.

A. Propagation Loss

Factor $h_{k,l}$ represents the attenuation in signal intensity as a result of absorption and scattering. Here, to simplify the derivation of analytical models for the link performance metrics, we approximate $h_{k,l}$ by the exponential attenuation model of Beer–Lambert, which neglects the multiple scattering effect [4, 6]

$$h_{k,l} = \exp(-Lc_e), \tag{3}$$

where c_e denotes the beam extinction coefficient for a collimated light source, e.g., a laser beam, in contrast to K_d, which is considered for a diffuse light source [20].

B. Oceanic Turbulence

Oceanic turbulence results from random variations of the refractive index along the aquatic medium, which causes fluctuations in the intensity and phase of the average received signal [21]. For a vertical UWOC link, these fluctuations are mostly due to the variations in water temperature and salinity with depth. Based on the profiles of temperature and salinity in the Argo database [22] for different geographical locations and over a long period of time, the log-normal PDF shows a good match with the majority of measured temperature and salinity gradients [23]. We, hence, model h_t by a log-normal distribution, that is

$$f_{h_t}(h_t) = \frac{1}{h_t\sqrt{2\pi\sigma_T^2}} \exp\left(-\frac{\left(\ln(h_t)-\mu_T\right)^2}{2\sigma_T^2}\right). \tag{5}$$

Note that other models have been proposed for the cases of moderate-to-strong turbulence, e.g., the gamma-gamma PDF in [24].

Following the approach in [25], and as illustrated in Fig. 2, the channel is considered a cascade of layers with different mean and variance turbulence parameters, which are assumed to be unchanged within each layer. Assume a total of K layers, with the k-th layer of thickness L_k (where $L = \sum_{u=1}^{U} L_u$), mean μ_{T_u}, and variance $\sigma_{T_u}^2$. The PDF of the corresponding channel coefficient h_{T_u} is

$$f_{h_{t_u}}(h_{t_u}) = \frac{1}{h_{t_u}\sqrt{2\pi\sigma_{T_u}^2}} \exp\left(-\frac{\left(\ln(h_{t_u})-\mu_{T_u}\right)^2}{2\sigma_{T_u}^2}\right). \tag{6}$$

The relationship between $\sigma_{T_u}^2$ and the scintillation index of the k-th layer $\sigma_{I_u}^2$ is given by [26]

$$\sigma_{T_u}^2 = 0.25\ln\left(1+\sigma_{I_u}^2\right) \approx 0.25\sigma_{I_u}^2 \quad \text{for} \quad \sigma_{I_u}^2 \square\ 1.$$

Note that this relationship is valid for the weak turbulence regime, i.e., for $\sigma_{I_u}^2 < 1$. Assuming independent, non-identically distributed h_{T_u}, μ_T, and σ_T^2 in Eq. (5) are [27]

$$\begin{cases} \mu_T = \sum_{u=1}^{U} 2\mu_{T_u}, \\ \sigma_T^2 = \sum_{u=1}^{U} 4\sigma_{T_u}^2. \end{cases} \tag{7}$$

To normalize the fading coefficient, i.e., to have $E\{h_{T_u}\} = 1$, we set $\mu_{T_u} = -\sigma_{T_u}^2$.

A well-known method to reduce the scintillation effect on the received signal is aperture averaging, by using an Rx aperture diameter D_r larger than the correlation width of the irradiance fluctuations ρ_c [28]. For a horizontal link and under weak turbulence conditions, the correlation width for a Gaussian beam is given by $\rho_c \sim \sqrt{L/K_w}$, where K_w is the wave number. A few previous works have studied the effect of aperture averaging for horizontal UWOC links [29–31]. To investigate the efficiency of aperture averaging in reducing the oceanic turbulence effect in the considered application scenario, we assume that the Rx uses a Gaussian lens, which is a combination of a thin lens with a Gaussian limiting aperture (i.e., a soft aperture) [31].

Assuming a large enough photodetector (PD) active area [30], to obtain the PDF of Eq. (5) while accounting for aperture averaging, first the scintillation indices $\sigma_{T_u}^2(D_r)$ corresponding to each of the u-th layer should be calculated in Eq. (B1) in Appendix B [13].

C. Beam Spreading Loss

At the receiver, a Gaussian beam profile and a circular detection aperture are assumed to quantify the effect of beam spreading. At the distance of L_{owc}, the normalized spatial distribution of optical intensity can be calculated as

$$I_{beam}(\rho_e; D) = \frac{2}{\pi\omega_D^2} \exp\left(-\frac{2\|\rho_e\|}{\omega_D^2}\right), \tag{8}$$

where ω_L is the beam size at the distance L_{owc}. ρ_e is the radial vector from the center of beam footprint and $\|.\|$ defines the expression of Euclidean norm. The beam spreading loss is quantified by the fraction of power collected by the detector $h_{bl}(.)$. It not only depends on the beam size but also the relative position between the centers of the detector and the beam footprint, which is known as pointing error. Denoting r as the pointing error, $h_{bl}(.)$ can be determined as

$$h_{bl}(r; D) = \int_A I_{beam}(\rho - r; D)\, d\rho, \tag{9}$$

where A is the area of detector. The Gaussian form of $h_{bl}(.)$ is written as

$$h_{bl}(r; D) \approx A_0 \exp\left(-\frac{2r^2}{\omega_{Leq}^2}\right), \tag{10}$$

where $\omega_{Leq}^2 = \omega_D^2(\sqrt{\pi}erf(v))/2v\exp(-v^2)$ defines the equivalent beam width at the destination. $A_0 = [erf(v)]^2$ and $v = \sqrt{\pi}a/\sqrt{2}\omega_D$ in which a is the radius of the detection aperture at the GS, r is the distance between the

center of the beam footprint and the detector. A_0 denotes the fraction of collected power at $r = 0$.

IV. SYSTEM PERFORMANCE ANALYSIS

At the receiver, the received signal is decoded using source #2's code $c_2(t)$. Assuming that chip-level synchronization is carried out, the decoded signal can be expressed as [32]

$$A_1 = \sum_{i=1}^{L} c_{2,i}^2(t)\, p(t - iT_c)\sqrt{P_2^R}\, \exp[\, j(\omega_c t + \varphi_2)] + \sum_{k=1,k\neq 2}^{K} \sum_{i=1}^{L} c_{k,i}(t) c_{2,i}(t)\, p(t - iT_c) \times \sqrt{P_k^R}\, \exp[\, j(\omega_c t + \varphi_2)]. \quad (11)$$

Theoretically, collected chips include not only the desired ones from source #2 but also the undesired ones from other sources considered as MAI. Next, the decoded signal is converted into an electrical signal by a photodetector (PD), where square-law detection is employed. The electrical signal is then integrated into a bit duration (T_b). The output signal from the integrator is written as

$$I = \frac{1}{T_b}\int_0^{T_b} \Re A_1 A_1^* dt = \Re\left(\rho P_2^R + \underbrace{\sum_{k=1,k\neq 2}^{K} X_k P_k^R}_{\text{MAI}}\right) + n(t), \quad (12)$$

where $\Re$ is the responsivity of the photodiode ρ is the code weight, which is corresponding to the number of chips "1" in $c_2(t)$. X_k is the cross-correlation value between two optical code $c_2(t)$ and $c_k(t)$. We consider the case that codes assigned to all GSs are selected from a code set. Accordingly, all X_k have the same value and we denote $X = X_k$.

Considering the effect of UWOC channel, the received signal at the destination from source #k including itself can be expressed as

$$P_k^R = P_k^T h_{k,l} h_{k,bl} h_t, \quad (13)$$

where h_t is the oceanic turbulence and $h_{k,l}$ is the propagation loss.

The mathematical expression of the received signal for the bit "1" and bit "0" at the input of the detector can be expressed as

$$I_1(m) = \Re(\rho + mX)P^R, \quad (14)$$

$$I_0(m) = \Re mXP^R, \quad (15)$$

where m is the number interfering sources that send simultaneously chip "1" at the detection chip.

The impact of the UWOC channel, MAI, and the impact of noise at the receiver are also considered in our analysis. Total noise that consists of shot noise, background noise, and thermal noise can be modeled as a Gaussian random variable with mean zero. Its variance for the case of bit "1" and bit "0" are given as

$$\sigma_1^2 = 2q(I_1 + \Re)B + \frac{4k_B T}{R_L} B, \quad (16)$$

$$\sigma_0^2 = 2q(I_0 + \Re)B + \frac{4k_B T}{R_L} B, \quad (17)$$

where q is the electronic charge, B is the equivalent noise bandwidth that is equal to the bit error rate (R_b) approximately, k_B is the Boltzmann's constant, T is the absolute temperature, and R_L is the load resistance.

The average bit error rate (BER) of the system can be written as

$$\text{BER} = \sum_{m=0}^{K-1} p(m)\text{BER}(m), \quad (18)$$

where BER(m) is the BER with m interfering sources. $p(m)$ is the probability that m of $K - 1$ interfering sources are simultaneously "1"s at the detection chip, which obeys the binomial distribution

$$p(m) = \binom{K-1}{m} 2^{1-K}. \quad (19)$$

Here, we assume that the probabilities of transmitting bit "0" and bit "1" of all sources are the same and equal to 1/2. Assuming that optimum threshold is used, the conditional probability of sending bit "1" and detecting bit "0" is equal to that of sending bit "0" and detecting bit "1". The BER hence can be calculated as

$$BER = \int_0^{\infty} f_{h_t}(h_t)\, Q\left(\frac{I_1(m) - I_0(m)}{\sigma_1 + \sigma_0}\right) dh_t. \quad (20)$$

V. RESULTS AND DISCUSSION

Table 1. System parameters

Name	Symbol	Value
Bolzmann's constant	k_B	1.38×10^{-23} $WHz^{-1}K^{-1}$
Electronic charge	q	$1.6x10^{-19}$ C
Light velocity	c	$3x10^8$ m/s
Load resistance	R_L	50 Ohm
Temperature	T	300 K
PD responsivity	$\Re$	0.8 A/W
Prime number	p	7
Packet length	N	5000 bits
Optical wavelength	λ	450 nm
Transmission distance	L_{owc}	20 – 25 m
Beam extinction coeff.	c_e	0.556 dB/m
Aperture radius	a	10 cm
Beam width	w_D	4 m

The numerical results are obtained and presented in this section based on the derived mathematical expressions. BER is evaluated versus the average received power ($P_{avg} = P_k^{(T)} h_{k,l}$) and the number of sources (K). In addition, the properties of the code set are also taken into account. First, the number of codes in a code set needs to be as many as the number of sources in the network. Second, to minimize MAI, the produced codes should have acceptable cross-correlation. The prime code in our analysis satisfies both the above requirements. For a prime number p from the Galois field, prime code (PC) has the length of p_2, the maximum cross-correlation of 1, the

weight of p, and the number of codes in a code set is p. Table 1 shows other system parameters whose values are fixed in our analysis. The following sequently introduces the results.

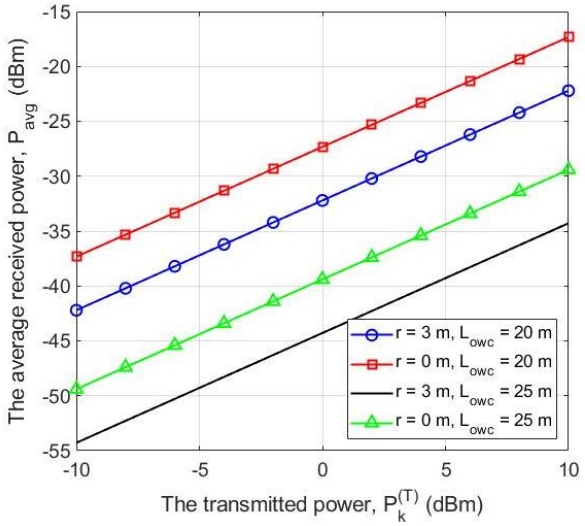

Fig. 3. The average received power versus the transmitted power with optical gain of 50 dB and receiver aperture radius of 10 cm.

First, Fig. 3 shows the relationship between the transmitted power versus the average received power with the optical gain of 50 dB at different values of pointing error. The purpose of the figure is to quantify the effect of two factors: propagation loss and beam spreading loss. When the effect of the pointing error is ignored, i.e., r = 0 m, the power loss can be determined based on the total of the link budget, i.e., the power difference between the transmitted power and the received power. For example, at the point that the transmitted power is −7.5 dBm and the received power is −30 dBm, the link budget is 22.5 dB, and thus the power loss is 72.5 dB, considering that the total gain is 50 dB. As pointing error causes the additional power loss, higher transmitted power is required to keep the received power unchanged.

All figures from now on are obtained based on the assumption that the misalignment, r, of 3 m. BER of a point-to-point system connecting between sources and destination is investigated versus the average received power when R_b is fixed at 10 Gbps (see Fig. 4). Obviously, high received power helps to mitigate the impacts of noise, interference, and atmospheric turbulence; thus, BER reduces with the increase of average received power. In addition, the system with a large code weight (i.e., $\rho = 19$) has lower BER than that of the one using a small code weight (i.e., $\rho = 7$). This is because the received power from the desired source is in proportion to the code weight. Last but not least, the impact of MAI presented via the number of underwater sensors, submarines, etc., can be evaluated in the figure, even though BER characteristics for the cases of 3 sources and 9 sources are slightly different due to the low cross-correlation of prime code.

In Fig. 5, BER is also evaluated in relation to the average received power. However, this figure focuses on only the impact of the bit rate while the number of sources is fixed to 9. The design of source's receiver is considered to make its BER controlled to meet the required targets. More specifically, BER is kept lower or equal to 10^{-3} so that bit errors can be corrected by error correction codes. Based on this requirement, the minimum received power (or the receiver sensitivity) can be determined. For instance, the minimum received power is −25 dBm when the bit rate is 10 Gbps. Clearly, the minimum received power is reduced when the bit rate decreases. This is because the bit rate governs the noise power via the equivalent noise bandwidth.

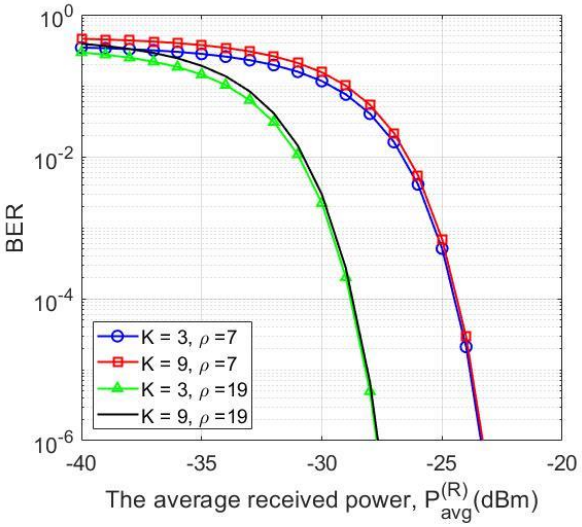

Fig. 4. BER versus the average received power with transmission rate of 10 Gbps.

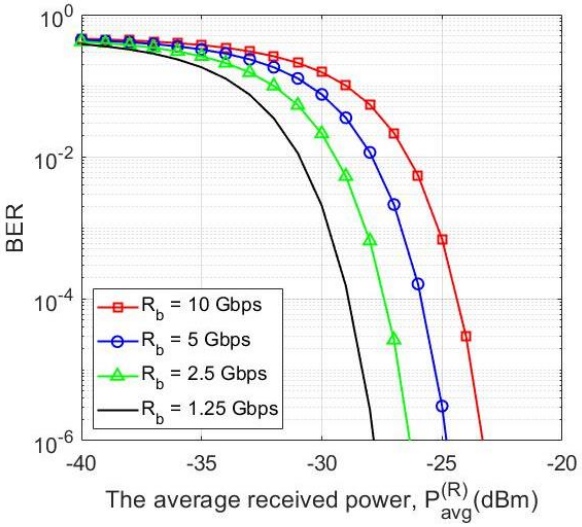

Fig. 5. BER versus the average received power when ρ = 7 and K = 9.

Some useful information for system design is to determine the number of supported sources corresponding to a specific value of the minimum received power (at BER $\leq 10^{-3}$) and the bit rate. This information can be obtained from Fig. 6, where prime code with p = 7 is used. When the minimum received power increases to −30 dBm, zero source can be supported with any transmission bit rate. When the minimum received power is −25 dBm, the network can support more than 8 sources with the bit rate of 10 Gbps.

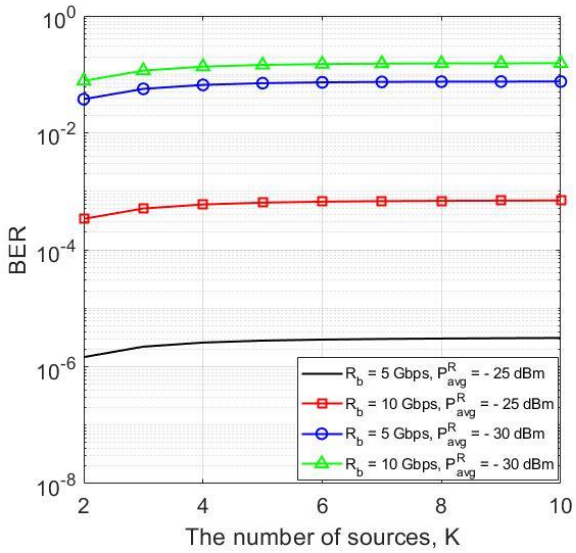

Fig. 6. BER versus the number of sources with code weight of 7.

VI. CONCLUDING REMARK

We considered a vertical UWOC link subject to propagation loss, beam spreading and pointing loss, oceanic turbulence-induced fading, MAI, and receiver noise investigated the BER performance of the link under different realistic operational conditions. Analytical expressions were derived for the link probability of bit error. The interest in optimum parameter selection for the Tx/Rx was further investigated, allowing significant performance improvement by making a compromise, especially regarding the effects of adverse issues. Furthermore, we investigated CDMA in UWOC system which is improved by reducing the effect of MAI. Based on an accurate mathematical expression for optical channel modeling that taking into account channel parameters under the effects of the propagation loss, oceanic turbulence-induced fading and beam spreading loss conditions. Furthermore, we provide an analytical expression for computing the bit error rate (BER). The numerical results give valuable insight into the practical aspects of the implementation of UWOC networks using CDMA for the future six-generation (6G) network.

The extension of this study to the case of downlink transmission, i.e., from the AUV to the buoy, is the subject of future research, which is, nevertheless, less problematic. As a matter of fact, our choice of focusing on the uplink is justified by the fact that the surface platform is much more subject to inclinations and displacements compared to the underwater platform; therefore, the link performance is more considerably subject to beam spreading loss. It could be interesting to apply more mitigation techniques such as relay transmission scheme, diversity, hybrid acoustic/OWC system, etc., to enhance the system performance.

VII. ACKNOWLEDGEMENT

This research was funded by Qualcomm Technologies, Inc under Research Agreement number POS-458996 (SOW number POS-459341).

REFERENCES

[1] M. A. Khalighi, C. J. Gabriel, L. M. Pessoa, and B. Silva, "Underwater visible light communications, channel modeling and system design," in Visible Light Communications: Theory and Applications (CRC Press, 2017), pp. 337–372

[2] M. A. Khalighi, C. Gabriel, T. Hamza, S. Bourennane, P. Léon, and V. Rigaud, "Underwater wireless optical communication; recent advances and remaining challenges (Invited paper)," in IEEE International Conference on Transparent Optical Networks (ICTON), Graz, Austria, 2014.

[3] X. Sun, C. H. Kang, M. Kong, O. Alkhazragi, Y. Guo, M. Ouhssain, Y. Weng, B. H. Jones, T. K. Ng, and B. S. Ooi, "A review on practical considerations and solutions in underwater wireless optical communication," J. Lightwave Technol. 38, 421–431 (2020).

[4] B. Cochenour, L. Mullen, and J. Muth, "Temporal response of the underwater optical channel for high-bandwidth wireless laser communications," IEEE J. Ocean. Eng. 38, 730–742 (2013).

[5] M. Doniec, M. Angermann, and D. Rus, "An end-to-end signal strength model for underwater optical communications," IEEE J. Ocean. Eng. 38, 743–757 (2013).

[6] C. Gabriel, M. A. Khalighi, S. Bourennane, P. Léon, and V. Rigaud, "Monte-Carlo-based channel characterization for underwater optical communication systems," J. Opt. Commun. Netw. 5, 1–12 (2013).

[7] T. Hamza, M. A. Khalighi, S. Bourennane, P. Léon, and J. Opderbecke, "Investigation of solar noise impact on the performance of underwater wireless optical communication links," Opt. Express 24, 25832–25845 (2016).

[8] J. W. Giles and I. N. Bankman, "Underwater optical communication systems. Part 2: basic design considerations," in Military Communications Conference (MILCOM), Atlantic City, New Jersey, 2005, pp. 1700–1705.

[9] O. Korotkova, N. Farwell, and E. Shchepakina, "Light scintillation in oceanic turbulence," Waves Random Complex Media 22, 260–266 (2012).

[10] C. Gabriel, M. A. Khalighi, S. Bourennane, P. Léon, and V. Rigaud, "Misalignment considerations on point-to-point underwater wireless optical links," in IEEE OCEANS Conference, Bergen, Norway, 2013.

[11] S. Tang, Y. Dong, and X. Zhang, "On link misalignment for under- water wireless optical communications," IEEE Commun. Lett. 16, 1688–1690 (2012).

[12] A. S. Ghazy, S. Hranilovic, and M. A. Khalighi, "Angular MIMO for underwater wireless optical communications: link modelling and tracking," IEEE J. Ocean. Eng. 46, 1391–1407 (2021).

[13] I. C. Ijeh, M. A. Khalighi, M. Elamassie, S. Hranilovic, and M. Uysal, "Outage probability analysis of a vertical underwater wireless optical link subject to oceanic turbulence and pointing errors," IEEE/OSA J. Opt. Commun. Netw., vol. 14, no. 6, pp. 439 – 453, June, 2022.

[14] M. Elamassie and M. Uysal, "Vertical underwater visible light communication links: channel modeling and performance analysis," IEEE Trans. Commun. 19, 6948–6959 (2020).

[15] E. Zedini, H. M. Oubei, A. Kammoun, M. Hamdi, B. S. Ooi, and M.- S. Alouini, "Unified statistical channel model for turbulence-induced fading in underwater wireless optical communication systems," IEEE Trans. Commun. 67, 2893–2907 (2019).

[16] John G. Proakis, "Modulation and demodulation techniques for underwater acoustic communications," in the proceedings of the 1st ACM international workshop on Underwater networks, Sept. 2006.

[17] F. Akhoundi, J. A. Salehi, and A. Tashakori, "Cellular Underwater Wireless Optical CDMA Network: Performance Analysis and Implementation Concepts," IEEE Trans. Commun, vol. 63, no. 3, pp. 882 - 891, Mar. 2015.
[18] F. Akhoundi, M. V. Jamali, N. B. Hassan, H. Beyranvand, A. Minoofar, and J. A. Salehi, "Cellular Underwater Wireless Optical CDMA Network: Potentials and Challenges," IEEE Access, vol. 04, pp. 4254 - 4268, Aug. 2016.
[19] M. V. Jamali, F. Akhoundi, and J. A. Salehi, "Performance Characterization of Relay-Assisted Wireless Optical CDMA Networks in Turbulent Underwater Channel," IEEE Trans. Wireless Commun., vol. 15, no. 6, pp. 4104 - 4116, June 2016.
[20] C. Mobley, E. Boss, and C. Roesler, "Ocean optics web book" [Accessed 16 December 2021], http://www.oceanopticsbook.info/.
[21] H. Kaushal and G. Kaddoum, "Underwater optical wireless communication," IEEE Access 4, 1518–1547 (2016).
[22] "Global ocean data assimilation experiment (GODAE)" [Accessed 15 April 2022], https://nrlgodae1.nrlmry.navy.mil/index.html
[23] M. V. Jamali, A. Mirani, A. Parsay, B. Abolhassani, P. Nabavi, A. Chisari, P. Khorramshahi, S. Abdollahramezani, and J. A. Salehi, "Statistical studies of fading in underwater wireless optical channels in the presence of air bubble, temperature and salinity random variations," IEEE Trans. Commun. 66, 4706–4723 (2018).
[24] M. Elamassie and M. Uysal, "Vertical underwater visible light communication links: channel modeling and performance analysis," IEEE Trans. Commun. 19, 6948–6959 (2020).
[25] L. C. Andrews, R. L. Phillips, and C. Y. Hopen, Laser Beam Scintillation with Applications (SPIE, 2001).
[26] M.-A. Khalighi, N. Schwartz, N. Aitamer, and S. Bourennane, "Fading reduction by aperture averaging and spatial diversity in optical wireless systems," J. Opt. Commun. Netw. 1, 580–593, (2009).
[27] M. C. Gökçe and Y. Baykal, "Aperture averaging and BER for Gaussian beam in underwater oceanic turbulence," Opt. Commun. 410, 830–835 (2018).
[28] I. Toselli and S. Gladysz, "Improving system performance by using adaptive optics and aperture averaging for laser communications in oceanic turbulence," Opt. Express 28, 17347–17361 (2020).
[29] Y. Fu, C. Huang, and Y. Du, "Effect of aperture averaging on mean bit error rate for UWOC system over moderate to strong oceanic turbulence," Opt. Commun. 451, 6–12 (2019).
[30] L. C. Andrews and R. L. Phillips, Laser Beam Propagation through Random Media (2005).
[31] M.-A. Khalighi, N. Schwartz, N. Aitamer, and S. Bourennane, "Fading reduction by aperture averaging and spatial diversity in optical wireless systems," J. Opt. Commun. Netw. 1, 580–593 (2009).
[32] Hien T. T. Pham, Minh B. Vu, Hoa T. Le, Linh D. Truong, and Ngoc T. Dang, "HAP-aided two-way relaying for FSO access networks using optical CDMA," Optical Engineering 60(9), Sept. 2021.

ĐÁNH GIÁ HIỆU NĂNG CỦA MẠNG IoT QUANG KHÔNG DÂY DƯỚI NƯỚC SỬ DỤNG KỸ THUẬT CDMA

Tóm tắt- Độ tin cậy của mạng truyền thông quang không dây dưới nước (UWOC) bị ảnh hưởng nghiêm trọng bởi sự lan truyền chùm tia và suy hao hướng giữa máy phát (Tx) và máy thu (Rx). Ngoài ra, hiệu suất của hệ thống UWOC có thể bị ảnh hưởng bởi pha-đinh do nhiễu loạn đại dương do sự dao động của chiết suất nước do sự thay đổi của áp suất, nước và nhiệt độ. Trong bài báo này, chúng tôi nghiên cứu phân tích hiệu năng của liên kết UWOC theo phương thẳng đứng chịu sự suy hao lan truyền, sự lan truyền chùm tia và suy hao hướng, và sự nhiễu loạn của đại dương. Hơn nữa, chúng tôi khảo sát khả năng đa truy cập phân chia theo mã (CDMA), được sử dụng để cho phép truyền dữ liệu không đồng bộ và đồng thời giữa các nguồn (ví dụ: cảm biến dưới nước, tàu ngầm, thợ lặn, v.v.) và điểm đích, có thể là một con tàu, phao, phương tiện không người lái dưới nước, v.v. Nghiên cứu này dựa trên một mô hình toán học chính xác để lập mô hình liên kết đồng thời tính đến các thông số kênh và Tx / Rx thực tế dưới tác động của nhiễu loạn đại dương và điều kiện suy hao lan truyền búp sóng. Ngoài ra, chúng tôi cung cấp một biểu thức phân tích để tính tỷ lệ lỗi bit (BER). Hơn nữa, sự cần thiết của việc lựa chọn tham số Tx / Rx tối ưu được chứng minh để thỏa mãn chất lượng dịch vụ như BER. Các kết quả được trình bày cung cấp cái nhìn sâu sắc có giá trị về các khía cạnh thực tế của việc triển khai các hệ thống UWOC sử dụng CDMA.

Từ khóa- Truyền thông quang không dây dưới nước (UWOC), đa truy cập phân chia theo mã (CDMA), nhiễu loạn đại dương.

Nguyen Van Thang received B.E. from Posts and Telecommunications Institute of Technology (PTIT), Vietnam, in 2017. He obtained M.E. and Ph.D. degrees in Computer Science and Engineering from the University of Aizu (Japan) in 2019 and 2022, respectively. His current research interests include the aera of communication theory with a particular emphasis on modeling, design and performance analysis of hybrid FSO/RF systems, optical wireless communications, satellite communications. He is a graduate student member of IEEE.

Pham Thi Thuy Hien received the B.E. Degree from Hanoi University of Transport and Communications in 1999; and the M.E. and Ph.D. degrees in Telecommunication Engineering from Posts and Telecommunications Institute of Technology (PTIT) in 2005 and 2017, respectively. She has been working at the Department of Wireless Communications of PTIT since 1999. Dr. Pham is currently a senior lecturer at PTIT. Her present research interests are in the area of design and performance evaluation of optical and wireless communication systems.